Polyamorphism

DOI: 10.1002/anie.201302974

Pressure-Induced Polyamorphism and Formation of 'Aragonitic' Amorphous Calcium Carbonate**

Alejandro Fernandez-Martinez, Bora Kalkan, Simon M. Clark, and Glenn A. Waychunas*

Amorphous calcium carbonate (ACC) is a precursor to the crystalline phases of $CaCO_3$, commonly found in the earliest stages of biomineral development and as one of the metastable states formed during the inorganic precipitation of calcium carbonate crystalline polymorphs.[1] Its isotropic and hydrous moldable character allows many organisms to form very complex conformations of their shells or skeletons by taking advantage of these unique properties.[2] At least two different phases of biogenic ACC have been described to date: a highly hydrated phase with one water molecule per $CaCO_3$ unit, and an anhydrous phase that forms as a transient phase prior to crystallization to vaterite or calcite.[3,4] Recently, the existence of polyamorphism (the existence of a substance in different amorphous modifications, akin to polymorphism in crystalline materials) in synthetic hydrated ACC has been suggested based mainly on X-ray absorption spectroscopy (XAS) and nuclear magnetic resonance (NMR) data that show different local structures of ACC precipitated from solutions at different pH values: calcite-like ACC is obtained at pH $\approx$ 8.75 and vaterite-like ACC precipitates from solutions of pH $\approx$ 9.8 and higher.[5,6] In addition to these two amorphous polymorphs, other studies have shown hints of aragonite local order in ACC from shells of freshwater snails, based on XAS data that show Ca-O coordination numbers of approximately 9, the theoretical value of aragonite.[7,8] These results were reproduced in synthetic samples of ACC doped with Mg^{2+}, suggesting a role of this cation in the selection of the ACC amorphous polymorph.[9]

Herein we show the existence of pressure-induced polyamorphism in hydrated ACC, and the formation of "aragonitic" ACC upon a decrease of the molar volume. This result suggests a possible mechanism by which Mg^{2+}—a cation with smaller ionic radius than Ca^{2+}—modifies the local order of ACC to an aragonite-like order by contributing to decrease the molar volume of the amorphous phase. In addition, we report the first values of the bulk modulus and the density of ACC.

Experimental structure factors obtained from high-pressure X-ray diffraction experiments and fits to the experimental data using Reverse-Monte Carlo (RMC) modeling are shown in Figure 1a. The structure factors show the typical broad oscillations of an amorphous solid, with no apparent sign of crystallization within the range of pressures studied. Pressure-induced structural changes can be identified in the diffraction data by looking at the salient feature of the S(Q) function at 11.9 GPa (see small arrow in Figure 1a), and by plotting the position of the main diffraction peak at Q $\approx$ 3.3 Å^{-1} as a function of pressure (Figure 1b). A step-like transition is observed that can be fitted with a sigmoidal function centered at $P_c = 9.8 \pm 0.8$ GPa. Similar behavior is observed in high-pressure Raman data (Figure 2; see raw data in Figure S7 and S8). At ambient pressure four peaks are observed: a single peak at 1081 cm^{-1} corresponding to the υ_1 symmetric stretching mode of the carbonate C–O bond, two peaks at 756 and 694 cm^{-1} that correspond to the υ_4 in-plane bending of the carbonate molecule and a single broad peak at approximately 270 cm^{-1}.[10] This peak, corresponds to lattice modes, which include water and carbonate librations and translations (see a discussion about this mode in section S6 of the Supporting Information). When the pressure is increased, the stretching mode shifts linearly to higher wavenumbers, showing a change of slope at approximately 10 GPa. The compressibility of the υ_1 band for aragonite is 2.0(1) cm^{-1} GPa^{-1} and for calcite is 3.0(3) cm^{-1} GPa^{-1}.[11] The ACC υ_1 band has a compressibility of 4.3 cm^{-1} GPa^{-1} which is softer than either of the crystalline phases. The two υ_4 modes show different behaviors: the mode at 756 cm^{-1} stays constant except for a 'bump' between approximately 5 and 10 GPa, where it undergoes a stiffening followed by a softening, a behavior seen at the onset of phase transitions in other crystalline carbonates.[12] The mode at 694 cm^{-1} shifts to

[*] Dr. A. Fernandez-Martinez
Institut des Sciences de la Terre
CNRS & Universite Joseph-Fourier Grenoble I
B.P. 53X, 38041 Grenoble Cedex 9 (France)
E-mail: Alex.Fernandez-Martinez@ujf-grenoble.fr
Homepage: http://isterre.fr/alex-fernandez-martinez
Dr. B. Kalkan, Dr. S. M. Clark
Advanced Light Source, Lawrence Berkeley National Laboratory
1 Cyclotron Road, Berkeley, CA 94720 (USA)
Dr. S. M. Clark
Department of Earth and Planetary Sciences, Macquarie University
2109 NSW (Australia)
Dr. A. Fernandez-Martinez, Dr. G. A. Waychunas
Earth Sciences Division, Lawrence Berkeley National Laboratory
1 Cyclotron Road, Berkeley, CA 94720 (USA)

[**] The Advanced Light Source is supported by the Director, Office of Science, Office of Basic Energy Sciences, of the U.S. Department of Energy under Contract No. DE-AC02-05CH11231. This research used resources of the National Energy Research Scientific Computing Center, which is supported by the Office of Science of the U.S. Department of Energy under Contract No. DE-AC02-05CH11231. A.F.-M. and G.A.W. were partially supported as part of the Center for Nanoscale Control of Geologic CO_2, an Energy Frontier Research Center funded by the U.S. Department of Energy, Office of Science, Office of Basic Energy Sciences under Award Number DE-AC02-05CH11231. B.K. acknowledges support from IAEA,fellowship Code No.: TUR/10006. We thank Adam F. Wallace for fruitful discussions.

Supporting information for this article is available on the WWW under http://dx.doi.org/10.1002/anie.201302974.

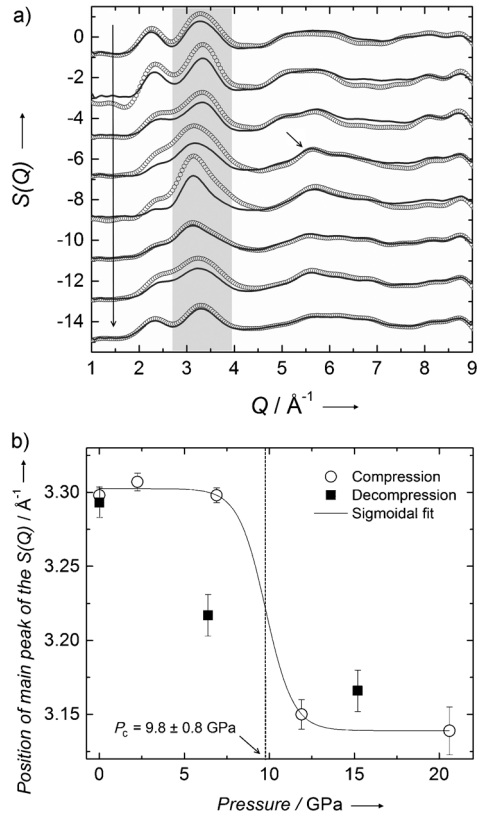

Figure 1. High-pressure X-ray scattering data. a) Experimental (black open circles) and modeled (lines) structure factors. The vertical arrow at the left indicates the time progression of the data as they were collected. The little arrow indicates a new feature in the structure factor appearing at 11.9 GPa. b) Plot of the position of the main diffraction peak (shown in gray in the top graph). Open circles indicate the position during compression, and black squares during decompression. A sigmoidal fit to the compression data is shown, with center (vertical dotted line) at $P_c = 9.8 \pm 0.8$ GPa.

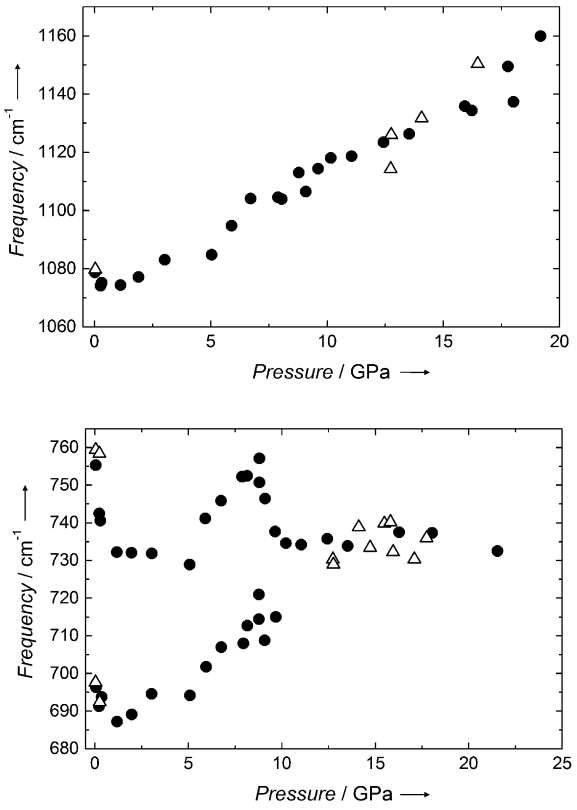

Figure 2. High-pressure Raman spectroscopy. The effect of pressure on the CO_3^{2-} symmetric stretching (υ_1) mode (top) and on the CO_3^{2-} in plane bending (υ_4) mode (bottom) in ACC. Closed circles denote data collected while increasing pressure and open triangles represent data collected while decreasing pressure.

higher wavenumbers, merging with the first υ_4 mode at approximately 10 GPa. For further increased pressures, only a single degenerate mode is observed. The intensity of the mode at approximately 270 cm^{-1} decreases with pressure, disappearing at a pressure of approximately 5 GPa, and reappearing upon decompression. The Ca–OH_2 stretching mode is usually visible in this region of the spectra; a plausible hypothesis is therefore that the disappearance of the peak is due to a change in the short-range order around the Ca ions at this pressure. These observations are indicative of a polyamorphic transition occurring at approximately 10 GPa. It is also interesting to see that the three modes at 1081, 756, and 694 cm^{-1} soften at low pressures. This effect has been observed in other systems, and has been interpreted as a loss of physisorbed surface water.[13] Interestingly, the whole transition and the surface dehydration process are reversible upon decompression of the material (see Figure 2).

The RMC analysis allows us to examine changes in the atomic pair correlations in detail, provided that the weight factor of the correlation of interest is high relative to other correlations in the structure (see sections S1.6 and S2 of the Supporting Information for a detailed explanation) as is the case for the Ca–Ca correlation in ACC. Figure 3a shows changes in the Ca–Ca partial pair distribution function (pPDF)—which is characteristic of the different $CaCO_3$ polymorphs—during compression up to 20.6 GPa and during decompression down to 0.3 GPa. At ambient pressure, a single broad correlation centered at approximately 4 Å is observed that splits into two different distances (ca. 3.95 Å and ca. 4.60 Å) as pressure is increased. Figure 3b shows a comparison between the ambient pressure Ca–Ca pPDF of ACC and those of the crystalline polymorphs, highlighting the good agreement with the pPDF of vaterite (red bold line in Figure 3; see a discussion about the ambient pressure structure of ACC in section S2 of the Supporting Information). The Ca–Ca pPDF of ACC at 11.9 GPa is shown in Figure 3c and compared to that of the three crystalline polymorphs at ambient pressure. The positions of the two first peaks are in good agreement with the Ca–Ca inter-atomic distances of aragonite (blue bold line). Also, the center of the broad Ca–Ca correlation at approximately 5.80 Å of ACC coincides with the center of the two peaks observed for aragonite. This result suggests that, at high pressures, the Ca atoms adopt a local-order configuration similar to that of aragonite, while keeping the amorphous character of the structure. The evolution of the coordination numbers under pressure confirms this result. At ambient pressure, 4.8 Ca^{2+} are found on average in the first shell, a number significantly

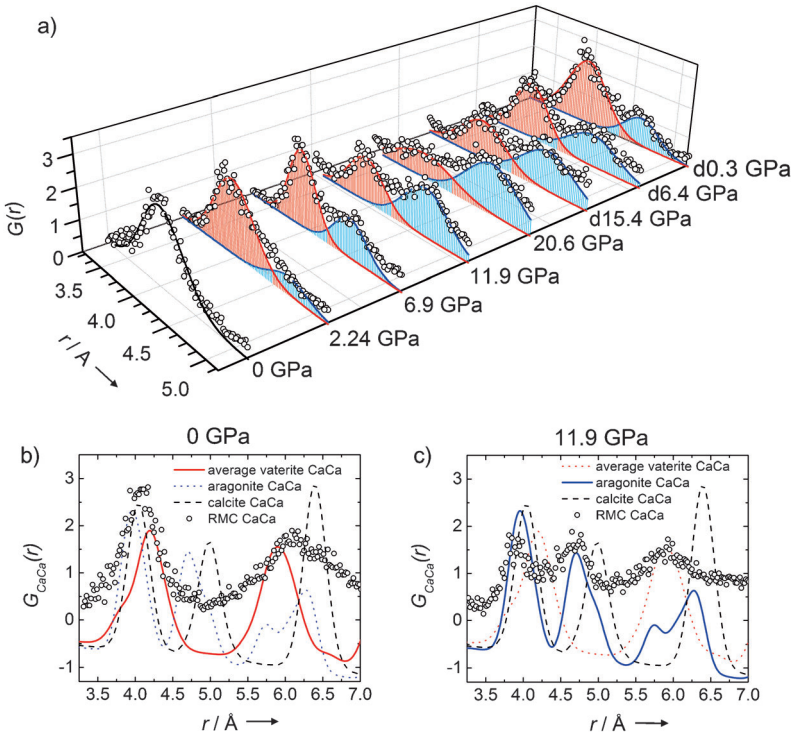

Figure 3. Evolution of the Ca–Ca correlation with pressure from reverse Monte-Carlo modeling. a) A single broad peak is observed at ambient pressure that splits into two different distances (red and blue) at high pressures. Pressure labels starting with "d" indicate data taken during decompression. b) Plot of the ACC Ca–Ca pPDF at ambient pressure, together with the pPDFs of calcite, aragonite, and vaterite at ambient pressure. c) Plot of the ACC Ca–Ca pPDF at 11.9 GPa, together with the pPDFs of calcite, aragonite and vaterite at ambient pressure. Note that the range of the *x*-axis is different in (a) and (b) and (c).

lower than the average of 6 found in calcite and in vaterite, but within the statistical distribution of values obtained from the RMC models.

This value increases to 10.2 at 20.6 GPa. This result is consistent with the formation of a local environment close to that of aragonite, which has 12 Ca^{2+} neighbors around each Ca^{2+}. The Ca–O coordination number shows a similar behavior, increasing from 6.5 to 8.2, which is close to the theoretical value of 9 for aragonite (a detailed description of the coordination number analysis is provided in section S5 of the Supporting Information).

The evolution of the molar volume measured using X-ray absorption is shown in Figure S11, together with a fit of a Birch–Murnaghan equation of state. From the fit a value for the bulk modulus of ACC of $K_{0\text{-compression}} = 27.2 \pm 1.4$ GPa has been obtained, which is significantly lower than that of the crystalline polymorphs (ranging from 67 to 72 GPa). A fit to the molar volume data during decompression yields a slightly different value of $K_{0\text{-decompression}} = 32.4 \pm 0.6$ GPa, indicating a small hysteresis. No appreciable difference has been found between the values of the zero-pressure molar volume for the low-pressure and high-pressure phases (see a detailed analysis of the molar volume data in section S3 of the Supporting Information). The value obtained for the zero pressure density is $\rho_{0\text{-ACC}} = 2.18\ \mathrm{g\,cm^{-3}}$.

Our X-ray scattering data, Raman data, and density measurements indicate the presence of an amorphous-to-amorphous phase transition in ACC at a critical pressure of about 10 GPa. RMC modeling of the structure of ACC constrained by our X-ray scattering data shows that, at high pressures, ACC forms a more compact phase with a local order compatible with a disordered aragonite or "aragonitic-ACC" (see section S4 of the Supporting Information for a description of the Ca-CO_3 complexes characteristic of the aragonite crystal structure). Not surprising is the fact that a similar transformation occurs in crystalline $CaCO_3$, where aragonite is the most stable polymorph at pressures higher than approximately 1.5 GPa (aragonite formation is hindered kinetically if calcite is compressed at room temperature due to the formation of calcite-I and calcite-II, but these two metastable phases transform readily to aragonite upon annealing).[14,15] In contrast to the crystalline system, the transition of ACC to aragonitic-ACC is observed at a higher pressure (ca. 10 GPa), and it is at least partially reversible, as indicated by the increased compressibility during decompression. This last point suggests an active role of water as a structural element of ACC, controlling its elastic properties (see further discussion in section S6 of the Supporting Information).

From a fundamental perspective, the observed structural transition is a good example of pressure-induced polyamorphism, a phenomenon that has been reported to occur in materials, such as amorphous ice,[16,17] amorphous phosphorous[18] or silica[19] (see Ref. [20] for a Review). These transitions are expected to occur in systems whose constituents can adopt different coordination environments, with the proportion of each of them varying as a function of the pressure or temperature. This is the central idea of the "two-phase model", that was used by Rapoport[21] to explain the unusual presence of maxima in melting curves or the negative initial slope of *P*–*T* melting curves observed in some systems, and has since been used to predict polyamorphism. The crystalline phases of $CaCO_3$ are a good example of polymorphism based on different coordination environments. To our knowledge, this is the first example of direct observation of an amorphous–amorphous phase transition in a solid ionic system. Interestingly, other solid ionic crystalline phases, such as hydroxyapatite and gypsum, have been reported to form via hydrated amorphous precursors,[22,23] and hydrated amorphous phases with compositions similar to those of other crystalline carbonates siderite ($FeCO_3$), magnesite ($MgCO_3$), and dolomite ($MgCa(CO_3)_2$) have been discovered recently.[24,25] Given the existence of multiple crystalline polymorphs for some of these (such as the diversity of hydrated magnesium carbonates phases, reflecting multiple potential minima in their potential energy surfaces), it seems logical to expect that

polyamorphism could occur, provided that the range of metastability of these amorphous phases extends to high pressures.

The observation that ACC adopts an aragonite-like local order when confined in a lower molar volume gives some hints about possible formation mechanisms of an amorphous precursor for aragonite. The poisoning of calcite growth in aqueous solutions enriched in Mg^{2+} or in sea water, and the subsequent precipitation of aragonite—whose growth does not seem to be affected by the presence of Mg^{2+}—have been widely documented.[26–28] Nonetheless, it is possible that Mg^{2+} has an effect other than as calcite growth inhibitor, exerting a direct control over the local structure of Mg^{2+}-rich ACC. Actually, relatively high concentrations of Mg^{2+} in solution were used in the only study that reports a synthetic ACC phase with aragonite local order around Ca^{2+} (local order was described using Ca^{2+} K-edge X-ray absorption spectroscopy).[9] The shorter Mg^{2+} ionic radius with respect to Ca^{2+} seems to be inducing a lower molar volume of the amorphous precursor—the same way as magnesian calcites have molar volumes lower than calcite—favoring an aragonite-like environment such as that observed in this study at high pressures.[29–31] More research is needed to ascertain the role of Mg^{2+} in controlling ACC polyamorphism.

Experimental Section

Briefly, amorphous calcium carbonate samples were prepared following the method reported by Koga et al.,[32] mixing 100 mL of $CaCl_2$ (0.02 M) with 100 mL of a solution containing Na_2CO_3 (0.02 M) and NaOH (0.2 M), and quickly drying under vacuum. High pressure X-ray diffraction and absorption experiments were performed using an asymmetric diamond anvil cell at beamline 12.2.2 of the Advanced Light Source.[33] The evolution of the density under pressure was determined using the method of Shen et al.[34,35] Reverse-Monte Carlo analysis of the scattering data was performed using the code RMCProfile.[36] Raman data were collected at a range of pressures from ambient to about 21.5 GPa using the microRaman system located at sector 6 of the Advanced Photon Source operated by GSE-CARS. A detailed Experimental Section is given in section S1 of the Supporting Information.

Received: April 10, 2013
Published online: July 1, 2013

Keywords: amorphous materials · calcium carbonate · phase transitions · Raman spectroscopy · X-ray diffraction

[1] Y. Politi, R. A. Metzler, M. Abrecht, B. Gilbert, F. H. Wilt, I. Sagi, L. Addadi, S. Weiner, P. U. P. A. Gilbert, *Proc. Natl. Acad. Sci. USA* **2008**, *105*, 17362 – 17366.
[2] L. Addadi, S. Raz, S. Weiner, *Adv. Mater.* **2003**, *15*, 959 – 970.
[3] Y. Politi, T. Arad, E. Klein, S. Weiner, L. Addadi, *Science* **2004**, *306*, 1161 – 1164.
[4] Y. U. T. Gong, C. E. Killian, I. C. Olson, N. P. Appathurai, A. L. Amasino, M. C. Martin, L. J. Holt, F. H. Wilt, P. U. P. A. Gilbert, *Proc. Natl. Acad. Sci. USA* **2012**, *109*, 6088 – 6093.
[5] D. Gebauer, P. N. Gunawidjaja, J. Y. P. Ko, Z. Bacsik, B. Aziz, L. Liu, Y. Hu, L. Bergström, C.-W. Tai, T.-K. Sham et al., *Angew. Chem.* **2010**, *122*, 9073 – 9075; *Angew. Chem. Int. Ed.* **2010**, *49*, 8889 – 8891.
[6] J. H. E. Cartwright, A. G. Checa, J. D. Gale, D. Gebauer, C. I. Sainz-Díaz, *Angew. Chem.* **2012**, *124*, 12126 – 12137; *Angew. Chem. Int. Ed.* **2012**, *51*, 11960 – 11970.
[7] B. Hasse, H. Ehrenberg, J. C. Marxen, W. Becker, M. Epple, *Chem. Eur. J.* **2000**, *6*, 3679 – 3685.
[8] J. C. Marxen, W. Becker, D. Finke, B. Hasse, M. Epple, *J. Molluscan Studies* **2003**, *69*, 113 – 121.
[9] R. S. K. Lam, J. M. Charnock, A. Lennie, F. C. Meldrum, *CrystEngComm* **2007**, *9*, 1226.
[10] U. Wehrmeister, D. E. Jacob, a. L. Soldati, N. Loges, T. Häger, W. Hofmeister, *J. Raman Spectrosc.* **2011**, *42*, 926 – 935.
[11] P. Gillet, C. Biellmann, B. Reynard, P. McMillan, *Phys. Chem. Miner.* **1993**, *20*, 1 – 18.
[12] R. Minch, L. Dubrovinsky, A. Kurnosov, L. Ehm, K. Knorr, W. Depmeier, *Phys. Chem. Miner.* **2009**, *37*, 45 – 56.
[13] S. A. Parry, A. R. Pawley, R. L. Jones, S. M. Clark, *Am. Mineral.* **2007**, *92*, 525 – 531.
[14] W. D. Carlson in *Reviews in Mineralogy and Geochemistry. Carbonates: Mineralogy and Chemistry*, Mineralogical Society of America, Chantilly, VA, USA, **1990**, p. 399.
[15] L.-G. Liu, T. P. Mernagh, *Am. Mineral.* **1990**, *75*, 801 – 806.
[16] O. Mishima, L. D. Calvert, E. Whalley, *Nature* **1985**, *314*, 76 – 78.
[17] J. Finney, A. Hallbrucker, I. Kohl, A. Soper, D. Bowron, *Phys. Rev. Lett.* **2002**, *88*, 225503.
[18] J. M. Zaug, A. K. Soper, S. M. Clark, *Nat. Mater.* **2008**, *7*, 890 – 899.
[19] D. Lacks, *Phys. Rev. Lett.* **2000**, *84*, 4629 – 4632.
[20] P. F. McMillan, M. Wilson, M. C. Wilding, D. Daisenberger, M. Mezouar, G. Neville Greaves, *J. Phys. Condens. Matter* **2007**, *19*, 415101.
[21] E. Rapoport, *J. Chem. Phys.* **1967**, *46*, 2891.
[22] A. S. Posner, F. Betts, *Acc. Chem. Res.* **1975**, *8*, 273 – 281.
[23] Y.-W. Wang, Y.-Y. Kim, H. K. Christenson, F. C. Meldrum, *Chem. Commun.* **2011**, *48*, 1 – 3.
[24] O. Sel, A. V. Radha, K. Dideriksen, A. Navrotsky, *Geochim. Cosmochim. Acta* **2012**, *87*, 61 – 68.
[25] A. V. Radha, A. Fernandez-Martinez, Y. Hu, Y. S. Jun, G. A. Waychunas, A. Navrotsky, *Geochim. Cosmochim. Acta* **2012**, *90*, 83 – 95.
[26] R. A. Berner, *Geochim. Cosmochim. Acta* **1975**, *39*, 489 – 504.
[27] R. Folk, *J. Sediment. Res.* **1974**, *44*, 40 – 53.
[28] N. De Leeuw, *Am. Mineral.* **2002**, *87*, 679 – 689.
[29] J. Paquette, R. J. Reeder, *Am. Mineral.* **1990**, *75*, 1151 – 1158.
[30] P. L. Althoff, *Am. Mineral.* **1977**, *62*, 772 – 783.
[31] J. Titschack, F. Goetz-Neunhoeffer, J. Neubauer, *Am. Mineral.* **2011**, *96*, 1028 – 1038.
[32] N. Koga, Y. Z. Nakagoe, H. Tanaka, *Thermochim. Acta* **1998**, *318*, 239 – 244.
[33] M. Kunz, A. A. MacDowell, W. A. Caldwell, D. Cambie, R. S. Celestre, E. E. Domning, R. M. Duarte, A. E. Gleason, J. M. Glossinger, N. Kelez et al., *J. Synchrotron Radiat.* **2005**, *12*, 650 – 658.
[34] X. Hong, G. Shen, V. B. Prakapenka, M. L. Rivers, S. R. Sutton, *Rev. Sci. Instrum.* **2007**, *78*, 103905.
[35] G. Shen, N. Sata, M. Newville, M. Rivers, *Appl. Phys. Lett.* **2002**, *81*, 1411 – 1414.
[36] M. G. Tucker, D. A. Keen, M. T. Dove, A. L. Goodwin, Q. Hui, *J. Phys. Condens. Matter* **2007**, *19*, 335218.

